applied sciences

MDPI

Article

Modelling Wave Transmission for Transient Flow and Amplitude-Frequency Characteristics of Tubular String in a Water Injection Well

Eryang Ming [1], Cong Li [2,*], Huiqing Lan [2,*], Jiaqing Yu [1], Lichen Zheng [1] and Xiaohan Pei [1]

[1] Research Institute of Petroleum Exploration & Development, PetroChina Company Limited, Beijing 100083, China
[2] Key Laboratory of Vehicle Advanced Manufacturing, Measuring and Control Technology, Ministry of Education, Beijing Jiaotong University, Beijing 100044, China
* Correspondence: 20116035@bjtu.edu.cn (C.L.); hqlan@bjtu.edu.cn (H.L.)

Abstract: Fluid wave code communication is used in layered water injection intelligent monitoring systems, but a model of fluid transient flow wave signal transmission is still unknown. Impedance and transfer coefficient in power transmission theory were used to describe transient flow waves in the transmission process of a tubular string in a water injection well and a transient flow wave model was built based on the transfer matrix method. The relationship between pressure and discharge was analyzed when the transient flow waves moved along the tubular string, and the influence of terminal impedance and dip angle of the tubular string on the wave transmission was studied. Simulations showed that the transient flow waves were with standing wave distribution when the transient flow wave signals transmitted in the tubular string. Moreover, the transmission volatility under different terminal impedances was analyzed. The communication frequency was selected according to the wave amplitude ratio between the two ends of the water injection tubular string. The relationship between the influence of tubular string parameters and fluid characteristics on the wave velocity and wave amplitude in the signal transmission process was obtained by simulation analysis. The wave velocity tended to decrease as the gas content increased. As the tube diameter–thickness ratio increased, the wave velocity decreased. Taking data from a water injection well in Daqing Oilfield as an example, a two-layer water injection test platform was built to study the fluctuation of discharge and pressure at monitoring points in the tubular string. The experiment condition was that the depth of the injection well was 1400 m. It was verified by the experiments that the pressure and flow changes in the downhole and wellhead had good consistency during the transmission of transient flow waves. Comparing the experimental results with the numerical results, the errors of the wave velocity and wave amplitude were 0.69% and 3.85%, respectively, indicating the verification of the simulation model. This study provides a theoretical support for the transmission of transient flow wave signals in a water injection tubular string.

Keywords: stratified water injection; transient flow wave; amplitude-frequency characteristics; transfer matrix

Citation: Ming, E.; Li, C.; Lan, H.; Yu, J.; Zheng, L.; Pei, X. Modelling Wave Transmission for Transient Flow and Amplitude-Frequency Characteristics of Tubular String in a Water Injection Well. *Appl. Sci.* **2023**, *13*, 3917. https://doi.org/10.3390/app13063917

Academic Editors: Jan Vinogradov, Ali Habibi and Zhengyuan Luo

Received: 15 February 2023
Revised: 17 March 2023
Accepted: 17 March 2023
Published: 19 March 2023

1. Introduction

Water flooding technology is widely used to improve oil recovery efficiency in oilfields [1,2]. The accurate control of the water injection rate for stratified water injection is a key issue in water injection technology [3–5]. Intelligent stratified water injection technology without ground mechanical operations has been gradually carried out at home and abroad [6]. Reliable and efficient wireless intelligent measurement has become a core technology in the field of water injection wells. In particular, data transmission technology is the most important part in wireless intelligent measurement technology. Using acoustics to transmit data in tubular strings has been reported, but the severe water and energy losses

in these systems has indirectly resulted in the insufficiency and inefficiency of these existing techniques [7]. There have been many applications for using transient flow transmission signals to detect pipe blockages and leaks [8–10]. Using transient flow waves to transmit signals is an effective way to control water injection and provide real-time guidance and optimization for wireless intelligent measurement and regulation.

Signal transmission techniques using transient flow have been developed and demonstrated in the engineering field [11,12]. It is well known that the transient wave transmission signal method is simple to operate. Moreover, the technology is economically efficient and can provide timely intelligent measurement and adjustment optimization decisions [6]. The drilling fluid pulse in measurement with drilling (MWD) is a typical transient flow wave communication method. It was developed in the late 1960s, matured and began to be used commercially in the 1970s [13]. At the beginning, transient flow wave communication technology was applied to layered oil production and water detecting/plugging on a small scale. In the late 2010s, it was applied to separated zone water injection, forming a transient flow wave-controlled separated zone water injection technology [13].

The theory of transient flow wave (water hammer) has been well developed, especially by the valuable research contributed by Joukowsky and Allievi. Joukowsky [14] produced the best-known equation in transient flow theory called the "fundamental equation of water hammer". Allievi [15] developed a general theory of water hammer from first principles and showed that the convective term in the momentum equation was negligible. He introduced two important dimensionless parameters widely used to characterize pipelines and valve behavior. Further refinements to the governing equations of water hammer appeared in Wood [16] and Streeter and Wylie [17]. Their combined efforts have resulted in the following classical mass and momentum equations for one-dimensional (1D) water hammer. For continuous transient flow waves in pipelines, Ham proposed the use of transfer functions to describe the transmission process of fluctuations. However, Ham's model is based on a simplified vibration model, and the error is relatively large when calculating long pipes [18]. Due to the low flow velocity of the injection tube, the generation and transmission of transient flow wave signals in the injection tube are different from that in measurement with drilling. Therefore, it is significant to study the model of the transient flow wave in a water injection tubular string.

During the water injection process, the tubular string can be considered as a vertical hollow tube. A mechanical device is used to generate the transient flow wave at the bottom of the well, and the wave signal is encoded. Then, the wave signal is transmitted by the tubular string, measured and decoded on the wellhead. Therefore, usage of the transient flow waves can pass the downhole measurement information to the wellhead [19]. However, the propagation mechanism of the transient flow wave is complicated [20]. Many scholars have studied the propagation mechanism and coding method of the transient flow wave signal [21,22]. However, because the signal transmission in the tubular string is affected by many factors, these influences need to be further studied for propagation mechanisms for transient flow wave signals. It is necessary to find better mathematical models to describe the transmission process and amplitude-frequency characteristics of transient flow waves. The model proposed in this paper can more accurately describe the transient flow wave transmission characteristics in the tubular string of water injection wells.

The transient flow wave characteristic is very important in long-distance transportation and valve operation. Therefore, many experimental and numerical studies were conducted to prevent mistaken operation of valve switches and to ensure the safety of pipelines and pumps [23–25]. Based on the different pressure transient responses, corresponding algorithms are developed and applied for blockage or leak detection [26,27]. All the studies can help to understand the transient flow wave transmission behavior. However, the water hammer response characteristics of the wellbore system are different from those in the pipeline system. Thus, experiment and numerical studies are needed to explain the transient flow wave response characteristics in the wellbore system. Wang et al. [28] studied the transient flow wave signal in the water injector and verified the water hammer propagation model through

experiments. Choi et al. [29] conducted a comprehensive study of water hammer effects in injection wells under different design parameters and operating parameters using OLGA simulations. In addition, signal analysis of transient flow waves mentioned above is only considered in time or frequency domain. The transient flow wave transmission behavior is more complicated. Combining methods in both time and frequency domains can help to better understand the transient flow wave transmission in a complex system. The gap between this paper and previous studies is the analysis of transient flow waves using time and frequency domains in two dimensions. This combination is needed because wave attenuation mechanisms are frequency- and time-dependent [30].

In this paper, a two-dimensional transient flow wave analysis method in time and frequency domains is proposed. Meanwhile, the transient flow transmission characteristics of the wellbore system are sufficiently presented to accurately investigate the transient flow wave transmission in the wellbore system. First, based on the theory of transient flow, the matrix calculation model of the transient flow wave signal transmitted in the water injection tubular string is established. The transient flow wave signal distribution in the water injection tubular string under the average friction is analyzed. When the continuous transient flow wave signal is transmitted in the tubular string, if the starting pressure head amplitude and discharge amplitude are known, the amplitude of the pressure head and discharge at any position can be calculated. Second, through experiments and calculations, the transmission characteristics of the transient flow wave signal are verified in the water injection tubular string. The calculation method of wave velocity and attenuation are studied. Third, the frequency domain characteristics of the water injection tubular string is also analyzed. It provides theoretical support for the selection of signal frequency and signal transmission in the layered water injection process. This study can provide clear insights into the use of transient flow waves for intelligent measurement and regulation and improve accurate control of downhole water injection.

2. Model of the Transient Flow Wave in Water Injection Tubular String

2.1. Transient Flow Wave Equations

The classical water hammer equation consists of two governing differential equations [17], one is the momentum equation, and the other is the continuity equation. Expressed in terms of pressure head H and discharge Q as:

$$\begin{cases} \frac{\partial Q}{A\partial t} + \frac{Q}{A^2}\frac{\partial Q}{\partial x} + g\frac{\partial H}{\partial x} + \frac{\lambda Q|Q|}{2DA^2} = 0 \\ \frac{\partial H}{\partial t} + \frac{Q}{A}\frac{\partial H}{\partial x} + \frac{Q}{A}\sin\beta + \frac{a^2}{gA}\frac{\partial Q}{\partial x} = 0 \end{cases} \tag{1}$$

This equation is a typical nonlinear hyperbolic partial differential equation. In many literatures, it uses various methods to find its numerical solution [31]. However, the numerical solution alone is obviously not enough for the transmission of continuous transient flow wave signals. Furthermore, it cannot be used to describe the transmission situation of continuous waves in the water injection tubular string, nor can they be used to choose the carrier frequency used by the transmitted transient flow wave signal communication.

In most of the engineering applications, the convective acceleration terms, $\frac{Q}{A}\frac{\partial H}{\partial x}$ and $\frac{Q}{A^2}\frac{\partial Q}{\partial x}$, are small as compared to the other terms [32]. Therefore, ignoring these terms from the governing equations, we obtain

$$\begin{cases} \frac{1}{gA}\frac{\partial Q}{\partial t} + \frac{\partial H}{\partial x} + \frac{\lambda Q|Q|}{2gDA^2} = 0 \\ \frac{\partial H}{\partial t} + \frac{a^2}{gA}\frac{\partial Q}{\partial x} + \frac{\sin\beta}{A}Q = 0 \end{cases} \tag{2}$$

In steady-oscillatory flow, the instantaneous discharge Q and the instantaneous pressure head H, may be divided into two parts: $Q = Q_0 + Q'$ and $H = H_0 + H'$, where Q_0 = mean discharge; Q' = discharge deviation from the mean; H_0 = mean pressure head; and H' = pressure head deviation from the mean.

Since the mean flow and pressure head are time-invariant ($\frac{\partial Q_0}{\partial t} = 0$ and $\frac{\partial H_0}{\partial t} = 0$) and the mean flow is constant along the tubular length ($\frac{\partial Q_0}{\partial x} = 0$), $\frac{\partial Q}{\partial x} = \frac{\partial Q'}{\partial x}$, $\frac{\partial Q}{\partial t} = \frac{\partial Q'}{\partial t}$, $\frac{\partial H}{\partial t} = \frac{\partial H'}{\partial t}$ [32]. According to Equation (2), when the pressure head is stable, there is $\frac{\partial H_0}{\partial x} = -\frac{\lambda Q_0 |Q_0|}{2gDA^2}$.

Because $Q' \ll Q_0$, the higher-order term Q'^2 can be neglected and $\frac{\lambda(Q_0+Q')^2}{2gDA^2} \doteq \frac{\lambda Q_0{}^2}{2gDA^2} + \frac{\lambda Q_0 Q'}{gDA^2}$. It follows from Equation (2) that:

$$\begin{cases} \frac{\partial H'}{\partial x} + \frac{1}{gA}\frac{\partial Q'}{\partial t} + RQ' = 0 \\ \frac{\partial H'}{\partial t} + \frac{a^2}{Ag}\frac{\partial Q'}{\partial x} + \frac{\sin\beta}{A}Q' = 0 \end{cases} \tag{3}$$

where $R = \frac{\lambda Q_0}{gDA^2}$ for turbulent flow. If λ is unchanged during wave transmission, R represents the average resistance of fluctuations in the tubular string, which is the resistance of the tube when the fluid stabilizes. Equation (3) can be called the continuous transient flow wave equations in the tubular string.

2.2. Transient Flow Wave Transmission Model

The field matrix for a tube may be derived by using the separation-of-variable method [17]. Elimination of Q' from Equation (3) yields

$$\frac{1}{a^2}\frac{\partial^2 H'}{\partial t^2} - \frac{g\sin\beta}{a^2}\frac{\partial H'}{\partial x} + \frac{RgA}{a^2}\frac{\partial H'}{\partial t} - \frac{\partial^2 H'}{\partial x^2} = 0 \tag{4}$$

As a result, the differential equation of the pressure head about time and position is obtained for the water injection tubular string. It can be seen from Equation (4) that there is a continuous fluctuation of discharge and pressure head in any position in the tube. The solution of Equation (4) is:

$$H' = \left(c_1 e^{\gamma_1 x} + c_2 e^{-\gamma_2 x}\right) e^{\mathrm{j}\omega t} \tag{5}$$

where $H' = h(x)e^{\mathrm{j}\omega t}$, $h(x)$ represents the amplitude of the pressure head at the x, c_1 and c_2 are arbitrary constants, and ω = angular frequency in rad/s; $\mathrm{j}^2 = -1$. Equation (5) indicates that the pressure head in any position in the water injection tube can be regarded as a superposition of pressure head fluctuations in two different directions. The parameters γ_1 and γ_2 (as the transfer coefficients in the tubular string) can be calculated as:

$$\gamma_1 = \frac{\sqrt{g^2\sin^2\beta - 4(a^2\omega^2 - \mathrm{j}\omega RgAa^2)} - g\sin\beta}{2a^2} \tag{6}$$

$$\gamma_2 = \frac{\sqrt{g^2\sin^2\beta - 4(a^2\omega^2 - \mathrm{j}\omega RgAa^2)} + g\sin\beta}{2a^2} \tag{7}$$

The real part of γ_1 and γ_2 represents the attenuation of the amplitude during transmission, and the imaginary part represents the change of phase. $g\sin\beta$ represents the effect of gravity on the transient flow wave. For a vertical downhole string, there is $\sin\beta = 1$.

Derivative of Equation (5) for t:

$$\frac{\partial H'}{\partial t} = \mathrm{j}\omega e^{\mathrm{j}\omega t}\left(c_1 e^{\gamma_1 x} + c_2 e^{-\gamma_2 x}\right) \tag{8}$$

Substituting Equation (8) into the second formula of Equation (3) can obtain:

$$\frac{\partial Q'}{\partial x} + \frac{g\sin\beta}{c^2}Q' = -\frac{\mathrm{j}\omega gA}{c^2}\left(c_1 e^{\gamma_1 x} + c_2 e^{-\gamma_2 x}\right) e^{\mathrm{j}\omega t}$$

Thus Q' can be calculated:

$$Q' = \frac{\omega g A}{\mathrm{j}a^2}\left(\frac{c_1 e^{\gamma_1 x}}{\gamma_2} - \frac{c_2 e^{-\gamma_2 x}}{\gamma_1}\right)e^{\mathrm{j}\omega t} \tag{9}$$

Equation (9) shows that there is also a fluctuation of discharge in any position in the tubular string. In which $Q' = q(x)e^{\mathrm{j}\omega t}$, $q(x)$ represents the amplitude of the pressure head at the x.

In the tubular string, fluctuations in pressure head cause fluctuations in discharge. The hydraulic impedance $Z(x)$ in a water injection system is defined as the ratio of the complex head to the complex discharge at a particular point in the tube.

$$Z(x) = \frac{h(x)}{q(x)} = -\frac{a^2\gamma_1\gamma_2}{j\omega g A}\frac{c_1 e^{\gamma_1 x} + c_2 e^{-\gamma_2 x}}{(\gamma_1 c_1 e^{\gamma_1 x} - \gamma_2 c_2 e^{-\gamma_2 x})} \tag{10}$$

The impedance of an infinitely long tubular string can be defined as the characteristic impedance, and the characteristic impedance can be written [17]:

$$Z_c = \lim_{x\to\infty} -\frac{a^2\gamma_1\gamma_2}{j\omega g A}\frac{(c_1 e^{\gamma_1 x} + c_2 e^{-\gamma_2 x})}{(\gamma_1 c_1 e^{\gamma_1 x} - \gamma_2 c_2 e^{-\gamma_2 x})} = -\frac{a^2\gamma_2}{j\omega g A} \tag{11}$$

Equation (11) shows that the characteristic impedance is constant for a fixed frequency signal and represents the inherent influence of the tube on the transient flow wave signal at a certain frequency. For an infinitely long tubular string, the fluctuations are transmitted in only one direction of the wave, without the presence of reflected waves. For the integration constants c_1, c_2, which need to be found using the boundary conditions, they are related to the pressure head and discharge at the beginning of the fluctuation.

At $x = 0$, $h(0) = c_1 + c_2$, $q(0) = \frac{\omega g A}{ja^2}\left(\frac{c_1}{\gamma_2} - \frac{c_2}{\gamma_1}\right)$. Thus,

$$c_1 = \frac{\gamma_2}{\gamma_1+\gamma_2}h_0 + \frac{\gamma_1}{\gamma_1+\gamma_2}Z_c q_0,\ c_2 = \frac{\gamma_1}{\gamma_1+\gamma_2}h_0 - \frac{\gamma_1}{\gamma_1+\gamma_2}Z_c q_0 \tag{12}$$

The expressions for $h(x)$ and $q(x)$ can be written as:

$$h(x) = \left(\frac{\gamma_2}{\gamma_1+\gamma_2}e^{\gamma_1 x} + \frac{\gamma_1}{\gamma_1+\gamma_2}e^{-\gamma_2 x}\right)h(0) + Z_c\frac{\gamma_1}{\gamma_1+\gamma_2}\left(e^{\gamma_1 x} - e^{-\gamma_2 x}\right)q(0) \tag{13}$$

$$q(x) = \frac{1}{Z_c}\frac{\gamma_2}{\gamma_1+\gamma_2}\left(e^{\gamma_1 x} - e^{-\gamma_2 x}\right)h(0) + \left(\frac{\gamma_1}{\gamma_1+\gamma_2}e^{\gamma_1 x} + \frac{\gamma_2}{\gamma_1+\gamma_2}e^{-\gamma_2 x}\right)q(0) \tag{14}$$

Equations (13) and (14) illustrate that when the continuous transient flow wave signal is transmitted in the tubular string, if the starting pressure head amplitude and discharge amplitude are known, the amplitude of the pressure head and discharge at any position can be calculated.

2.3. Transient Flow Wave Transfer Matrix in a Water Injection Tubular String

The transfer matrix method is used for the analysis of steady oscillatory flows and the determination of the frequency response of hydraulic systems [17]. According to Equations (13) and (14), the transfer matrix of transient flow wave fluctuations in the tubular string can be defined, and the fluctuations of pressure head h_i and q_i at the beginning are used to define the fluctuations of pressure head h_x and discharge q_x at position x in the tubular string:

$$\begin{bmatrix} h_x \\ q_x \end{bmatrix} = \begin{bmatrix} A(x) & B(x) \\ C(x) & D(x) \end{bmatrix}\begin{bmatrix} h_i \\ q_i \end{bmatrix} \tag{15}$$

where

$$A(x) = \frac{\gamma_2}{\gamma_1+\gamma_2}e^{\gamma_1 x} + \frac{\gamma_1}{\gamma_1+\gamma_2}e^{-\gamma_2 x},\ B(x) = Z_c\frac{\gamma_1}{\gamma_1+\gamma_2}\left(e^{\gamma_1 x} - e^{-\gamma_2 x}\right) \tag{16}$$

$$C(x) = \frac{1}{Z_c}\frac{\gamma_2}{\gamma_1+\gamma_2}\left(e^{\gamma_1 x} - e^{-\gamma_2 x}\right),\ D(x) = \frac{\gamma_1}{\gamma_1+\gamma_2}e^{\gamma_1 x} + \frac{\gamma_2}{\gamma_1+\gamma_2}e^{-\gamma_2 x} \tag{17}$$

Equation (15) illustrates that matrix $\mathbf{M}_l = \begin{bmatrix} A(x) & B(x) \\ C(x) & D(x) \end{bmatrix}$ can be defined as the transfer matrix of a single tubular string. From the definition of $\mathbf{M}_l$, it is known that the determinant value is $|\mathbf{M}_l| = e^{(\gamma_1-\gamma_2)x} \neq 0$. So $\mathbf{M}_l$ must be reversible, indicating that if the end pressure head amplitude h_l, the discharge amplitude q_l and length l of a tubular string are known, the pressure head amplitude and discharge amplitude at any position can be calculated. The relationship among inputs h_i and q_i at the beginning and outputs of the tubular string, h_i and q_i at the end can be represented by a four-port model shown in Figure 1.

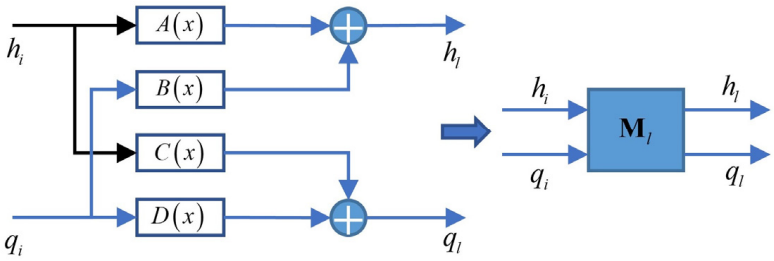

Figure 1. Single pipe four-port equivalence model.

A junction of two tubes that have different diameters, wall thicknesses, wall materials or any combination of these variables is called a series junction. It follows from the continuity equation with $q_l = q_i$ and $h_l = h_i$. The point transfer matrix for a series junction can be expressed as:

$$\mathbf{M}_D = \begin{bmatrix} 1 & 0 \\ 0 & 1 \end{bmatrix} \tag{18}$$

Since Equation (18) is a unit matrix, for a series connection of multiple tubes, the transfer matrix of the whole tubular string can be expressed as:

$$\mathbf{M}^* = \mathbf{M}_{l1}\mathbf{M}_{l2}\ldots\mathbf{M}_{ln} \tag{19}$$

The relationship between these series tubes can be represented by the multiple series four-port model shown in Figure 2.

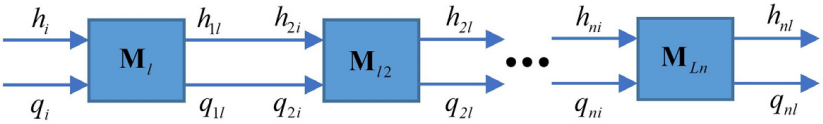

Figure 2. Four-port equivalent model when multiple tubes are connected in series.

When the continuous transient flow wave is transmitted in a series of tubes, according to the model shown in Figure 2 and Equation (19), the transmission matrix when multiple tubes are connected in series can be simplified to an equivalent transmission matrix $\mathbf{M}^*$ according to the matrix multiplication method, so that the transmission process can be expressed as:

$$\begin{bmatrix} p_l \\ q_l \end{bmatrix} = \mathbf{M}^* \begin{bmatrix} p_i \\ q_i \end{bmatrix} = \begin{bmatrix} A^* & B^* \\ C^* & D^* \end{bmatrix} \begin{bmatrix} p_i \\ q_i \end{bmatrix} \tag{20}$$

During the water injection process, if the downhole distributor is considered as the signal source, the transmission of the transient flow wave signal in the tubular string and the amplitude reaching the wellhead can be calculated by Equation (20).

3. Transient Flow Wave Transmission Characteristics in Tubular String

3.1. Transient Flow Wave Velocity in Tubular String

The wave velocity is related to the components of the fluid, the tube characteristic and the environmental parameters [13]. The wave velocity has been estimated from Korteweg's formula [33]; the expression of wave velocity can be derived from the continuity equation as well as the equation of motion.

$$a = \sqrt{\frac{K_e}{\rho}} \tag{21}$$

From the above theoretical study, it is clear that the main parameter that now determines the wave velocity is the apparent bulk modulus of elasticity of the system K_e.

$$\frac{1}{K_e} = \frac{1}{K_l}\left[1 + \psi\frac{K_l d}{Ee} + \beta_g\left(\frac{K_l}{K_g} - 1\right)\right] \tag{22}$$

Based on the total volume of the mixed fluid, the formula for the density of the transport fluid can be obtained. The solid content in the tubular string of the water injection well is negligible, and the density formula of the mixed fluid is as follows:

$$\rho = (1 - \beta_g)\rho_l + \beta_g\rho_g \tag{23}$$

The gas density is determined from the equation of state as:

$$\rho_g = \frac{P}{ZRT} \tag{24}$$

where P is the absolute pressure, Pa; Z is the compression coefficient of the actual gas; T is the temperature, K; and R is the gas constant, $R \doteq 287.4\ \mathrm{N \cdot m/K_g \cdot K}$.

The transient flow wave velocity in the tubular string is as follows:

$$a = \sqrt{\frac{K_e}{\rho}} = \sqrt{\frac{K_l/\rho}{1 + \psi\frac{K_l d}{Ee} + \beta_g\left(\frac{K_l}{K_g} - 1\right)}} = \sqrt{\frac{\frac{K_l}{(1-\beta_g)\rho_l + \beta_g\rho_g}}{1 + \psi\frac{K_l d}{Ee} + \beta_g\left(\frac{K_l}{K_g} - 1\right)}} \tag{25}$$

MATLAB software was used to analyze the relationship between the effects of different parameters on the signal of transient flow wave. Taking data from a water injection well in Daqing Oilfield as an example, the depth of a water injection well is 1400 m, the inner diameter of injection tube d is 25 mm, the wall thickness e is 3.5 mm, the average pressure in the injection well is 3 MPa, the average temperature is $t = 30\ ^\circ\mathrm{C}$ and the gas content is $\beta_g = 0.5\%$. The modulus of elasticity of the tube is $E = 2.1 \times 10^5$ MPa and the modulus of elasticity of water is $K_l = 2.04 \times 10^3$ MPa. The density of water is $\rho = 997.87\ \mathrm{kg/m^3}$. The specific heat ratio of the gas is m = 1.2, $K_g = mP$ = 1.2 × 30 = 36 MPa; the Poisson's ratio of the tube is 0.3. Only axial restraint is applied to the tube at the wellhead, $\psi = 1.1096$. The liquid density ρ_l and the gas density ρ_g depend on the pressure and temperature in the tubular string.

As shown in Figure 3, the pressure in the well has a large impact on the transmission rate. The higher the pressure, the greater the transmission rate. At constant pressure, the density of water and gas decreases with the increasing temperature, which in turn leads to a decrease in the density of the mixed water, resulting in an increase in wave velocity. The gas content has a significant impact on the compressibility of the water. A large gas content will have a large attenuation pulse amplitude. As shown in Figure 4, the wave velocity tends to decrease as the gas content increases. The diameter–thickness ratio only affects the

characteristics and support of the tube. As the diameter–thickness ratio increases, the wave velocity decreases.

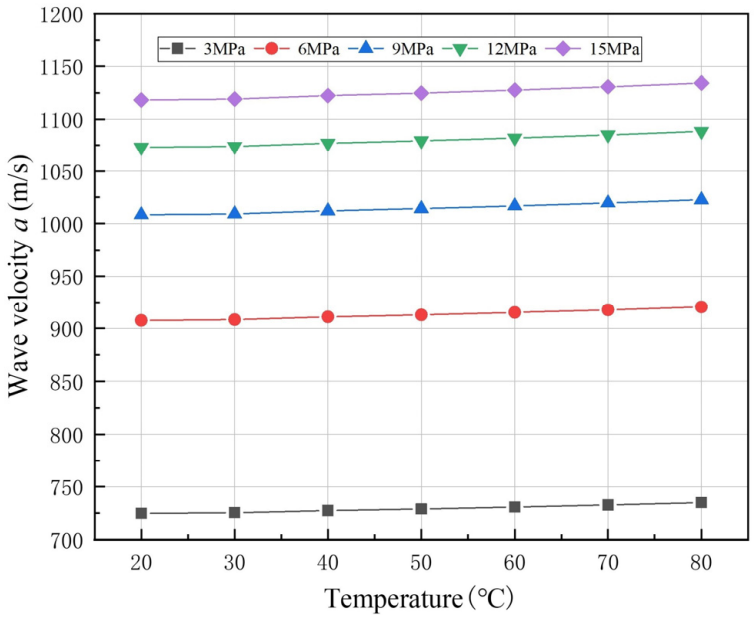

Figure 3. The effect of fluid temperature and pressure on wave velocity.

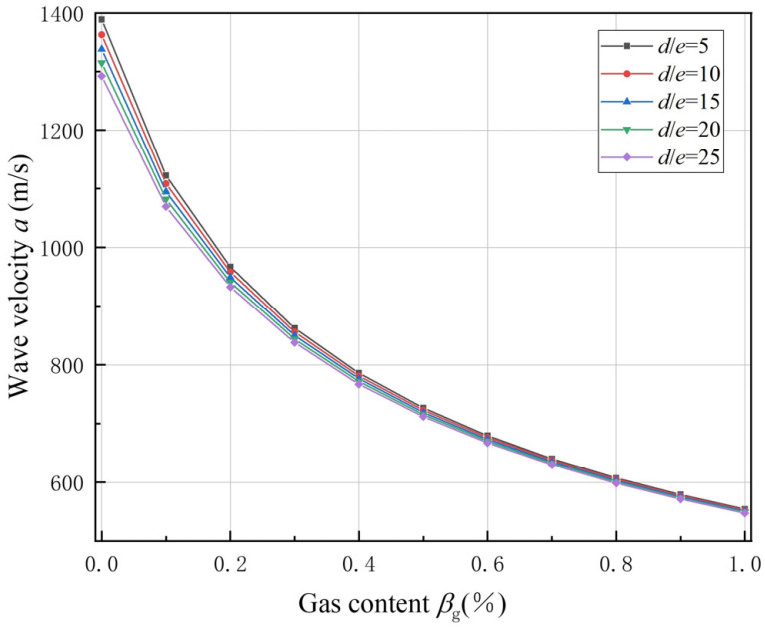

Figure 4. The effect of gas content and diameter–thickness ratio on wave velocity.

3.2. Transient Flow Wave Amplitude Attenuation in the Tubular String

The attenuation of the wave signal amplitude is related to the transmission distance of the signal in the tubular string and the characteristics of the transmission fluid. Most of the loss of transient flow wave transmission along the tubular string comes from the friction of the tube wall; the wave signal in the tubular string also conforms to the exponential attenuation law. According to Lambert's law [34], the quantitative relationship between the transmission characteristics of the wave signal in the tube, the amplitude of signal attenuation and the transmission distance in a tube filled with a mixture of fluids is expressed as:

$$P(x) = P_0 e^{-x/s} \tag{26}$$

Therefore, the transfer function is as follows:

$$H = \frac{P(x)}{P_0} = \exp(-x/s) \tag{27}$$

In which

$$S = \frac{aD}{2}\sqrt{\frac{\rho}{\pi f \omega}} \tag{28}$$

It follows from Equations (25) and (28) that

$$S = \frac{D}{2}\sqrt{\frac{K_l}{\pi f \omega\left[1 + \varphi\frac{K_l D}{Ee} + \beta_g\left(\frac{K_l}{K_g} - 1\right)\right]}} \tag{29}$$

where $P(x)$ is the pressure head at the transmission distance x, Pa; P_0 is the pressure head at the beginning, Pa.

This paper mainly analyzed the effects of temperature, signal frequency and gas content on the signal attenuation for transient flow waves, and $H = P(x)/P_0$ was used as an evaluation index of amplitude attenuation for signal waves. Three different temperatures 20 °C, 30 °C and 40 °C were selected for the transmission fluid (water). As can be seen from Figure 5, at a given transmission distance, the higher the temperature, the lower the signal attenuation. At the same temperature, as the transmission distance increases, the transmitted signal amplitude decreases exponentially with the transmission distance in a non-linear relationship. Because more energy is consumed the further the distance of pulse signal transmission, the received signal amplitude is relatively small.

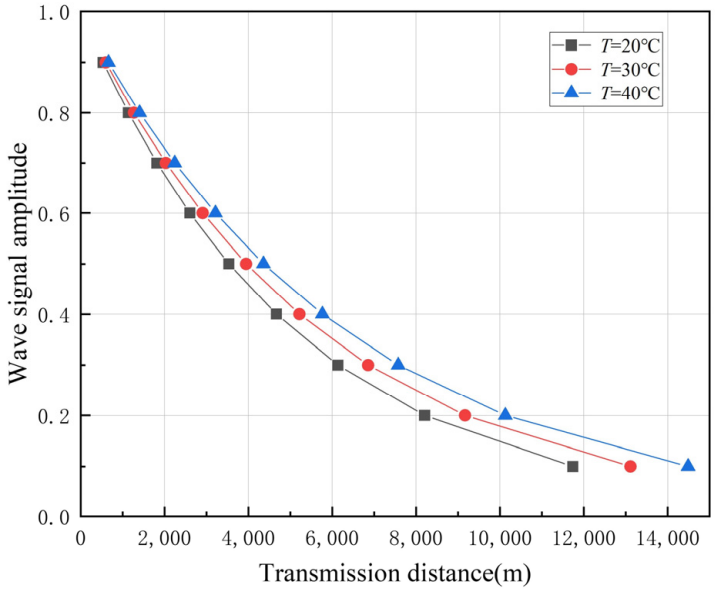

Figure 5. Effect of temperature on wave signal attenuation.

Three signals with different frequency 1 Hz, 2 Hz and 3 Hz were selected. From Figure 6, it can be concluded that the frequency causes a nonlinear near-exponential decrease in wave transmission amplitude with the transmission distance at the same distance. The higher the frequency, the smaller the signal amplitude.

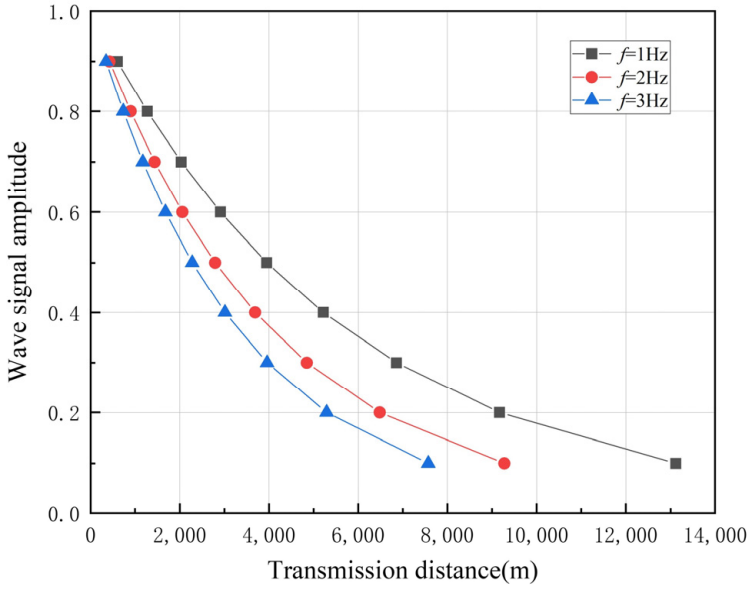

Figure 6. Effect of frequency on wave signal attenuation.

Three gas contents of 0.5%, 1.0% and 1.5% were selected for analysis. As shown in Figure 7, the increase in gas content dramatically decreases wave amplitude. The main reason is that when the wave encounters the gas in the dispersed phase, scattering loss is caused by the diffuse reflection at the interface due to the great difference of gas and liquid impedance.

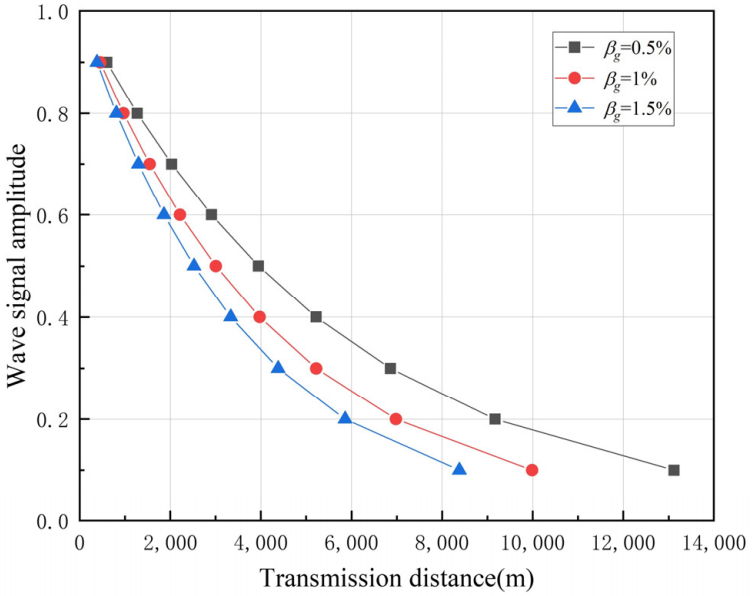

Figure 7. Effect of gas content on wave signal attenuation.

Attenuation of the wave amplitude is caused by two frequency-dependent mechanisms, fluid-related and scattering. The fluid-related mechanism is caused by the wave-induced frictional movement between fluid and tubular wall, known by wave-induced fluid flow (WIFF) [35]. Scattering, which is an elastic mechanism, is caused by heterogeneities in media; for instance, the heterogeneity caused by gas content in this case [36]. The gas content causes the two mechanisms since the compressibility of gas stimulates frictional losses and increases the heterogeneity. However, several studies have shown that when the gas content exceeds 5% the effect of gas on attenuation stagnates [37].

3.3. Transmission Characteristics Verification Experiment

In order to verify the accuracy of the transient flow wave velocity and wave attenuation calculation formula, an experiment was carried out, as shown in Figures 8 and 9.

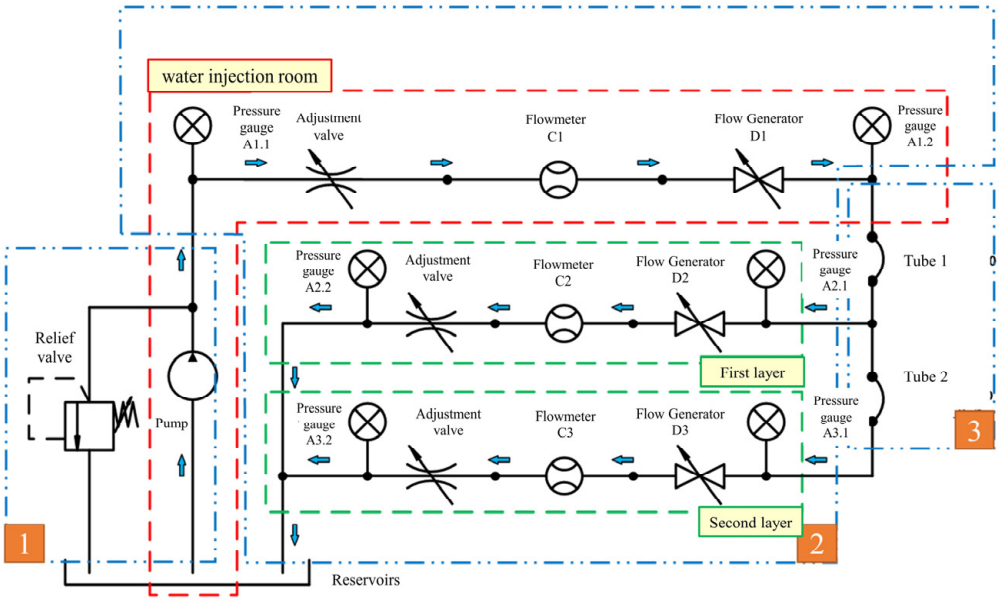

Figure 8. Diagram of two-layer stratified water injection test.

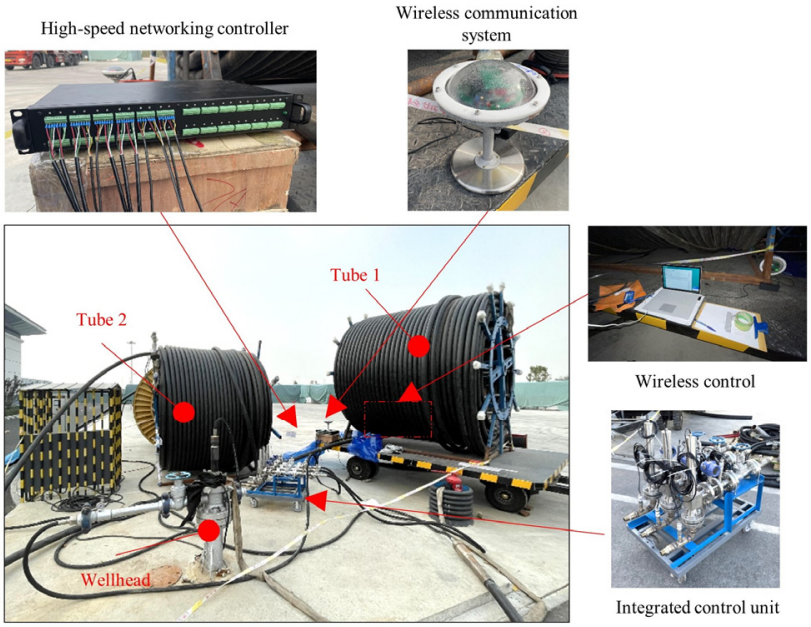

Figure 9. Two-layer stratified water injection test platform.

The experimental conditions were as follows: the depth of the injection well was 1400 m with a two-layered water injection, the length of the simulated tubular string from the water distribution room (injection room) to the first layer section was 1200 m, the length of the tubular string between the first layer and the second layer was 200 m. The test conditions are shown in Table 1. The gas density could be obtained from the equation of state as ρ_g = 34.43 kg/m^3. The specific heat ratio of the gas was m = 1.2; the Poisson's ratio of the tube was 0.3; only axial restraint was applied to the tube at the wellhead, φ = 1.1096.

Table 1. Two-layer stratified water injection test conditions.

Tube 1 Length (m)	Tube 2 Length (m)	Average Pressure (MPa)	Average Temperature (°C)	Gas Content (%)
1200	200	3	30	0.5

The procedure was as follows: Install the wave generator D1 at the beginning of the tube. It represents the transient flow wave signal at the wellhead generated by the variation of the ground valve opening. Install pressure sensor A1.2 near the wave generator D1 and record the measured pressure as p_0. Install flowmeter C1 near the wave generator and record the measured discharge as q_0. Similarly, install pressure sensor A3.1 near the wave generator D3 and record the measured pressure as p_2. Install flowmeter C3 near the wave generator D3 and record the measured discharge as q_2.

The control valve produced a continuous 'on–off' signal with a flow rate of 30 m^3/d. Stable transient flow fluctuations were generated in the pipeline and the values of p_0, p_2, q_0 and q_2 were recorded. The pressure and discharge fluctuation curves were plotted, and the test results are shown in Figures 10 and 11.

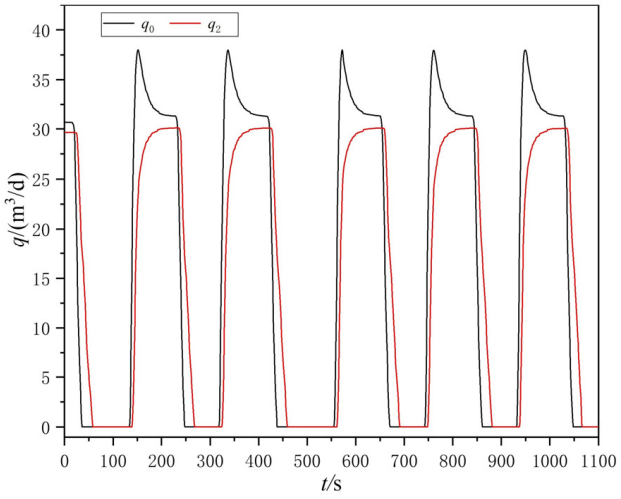

Figure 10. Transient discharge variation curves at upstream and downstream monitoring points.

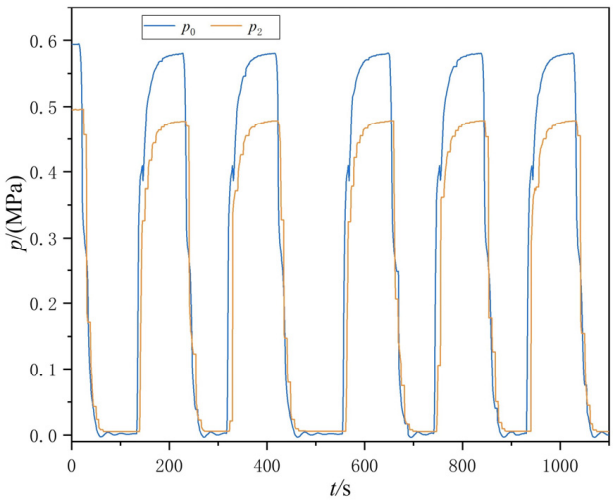

Figure 11. Transient pressure variation curves at upstream and downstream monitoring points.

The rise and fall attenuation time of the transient flow wave was about 1.9 s, which can be obtained experimentally. The wave transmission velocity can be obtained by Equation (25) as a = 725.27 m/s. Therefore, the transfer attenuation time was $t = l/a =$

1400/725.27 ≐ 1.93 s. Compared to the wave velocity test results with the calculated results, the error was 0.69%, indicating that the formula for calculating the fluctuation velocity of transient flow is correct.

The amplitude ratio of the monitoring point at 1400 m can be calculated by Equation (29) as $P(x)/P_0 = e^{(-x/s)} = e^{(-1400/5696.2)} \doteq 0.78$. The pressure values of the stable section at the upstream and downstream monitoring points were approximately 0.47 MPa and 0.58 MPa, in that order, and the ratio was $P_2/P_0 = 0.47/0.58 \doteq 0.81$. The error between the experimental value and the calculated value was 3.85%, which proves the correctness of the formula for calculating the attenuation of transient flow fluctuations.

4. Simulation of Transient Flow Wave Signals in Tubular Strings

4.1. Transient Flow Wave Signal Distribution along the Tubular String

During the water injection process, the modulated sinusoidal transient flow wave signals need to be transmitted from the well to the ground. The main concern in this process is the attenuation of the signal; the pressure fluctuation amplitude at the transmitting start point is p_i and the pressure fluctuation amplitude at the receiving point is p_l. The larger the p_l/p_i ratio, the stronger the received signal, and hence, the better signal transmission effect.

The ratio of the head amplitude h_l/h_i and the ratio of the pressure amplitude p_l/p_i at the two ends of the tubular string are equal. If defining $Z_l = h_l/q_l$ as a terminal impedance, according to Equations (16) and (17) it can be deduced:

$$\frac{h_l}{h_i} = \frac{p_l}{p_i} = \frac{A(l)D(l) - B(l)C(l)}{D(l) - B(l)\frac{1}{Z_l}} = \frac{e^{\gamma_l l - \gamma_2 l}}{D(l) - B(l)\frac{1}{Z_l}} \tag{30}$$

Equation (30) represents the value of amplitude transmission losses in the wave signal transmission. It can also be seen that the amplitude of the transient flow wave in the tubular string is influenced not only by the initial pressure head h_i, but also by the terminal impedance Z_l.

For a fixed frequency signal, it is assumed that the friction force is constant throughout the wave signal transmission process. The effect of the change in density of the gas content of the injection well fluid on the wave velocity is neglected. The effect of gas spillage on the signal is ignored, while the tubular string is considered rigid and its expansion and deformation during the transient flow wave transmission is ignored. Using the transfer matrix method derived earlier, the transfer process of the downhole continuous wave signal in the tubular string can be calculated.

According to the previous analysis, if the amplitude and frequency of pressure and discharge fluctuations at the begin of fluctuating signal are known, the amplitude of pressure and discharge fluctuations at any point in the tubular string can be calculated for a determined terminal impedance. Assume that the tube diameter D is 100 mm. The length l of the tubular string is 1500 m. The fluid viscosity is 3.81 mPa·s.

First, calculate the frictional resistance R, the transfer matrix $\mathbf{M}_l$ and the characteristic impedance Z_c. Set the terminal impedance value Z_l, and define the pressure value at position x between the beginning and the terminal as p_x; according to Equations (15) and (30), the following relationship can be obtained:

$$\frac{h_x}{h_i} = \frac{p_x}{p_i} = \frac{A(x)D(l) - \frac{1}{Z_L}A(x)B(l) - B(x)C(l) + \frac{1}{Z_l}A(l)B(x)}{D(l) - B(l)\frac{1}{Z_l}} \tag{31}$$

According to the matrix expression of Equation (12), when $x = l$, there is $A(l)D(l) - B(l)C(l) = e^{(\gamma_1 - \gamma_2)l}$. From Equation (31), the pressure wave amplitude distribution curve along the tubular string can be calculated, as shown in Figure 12.

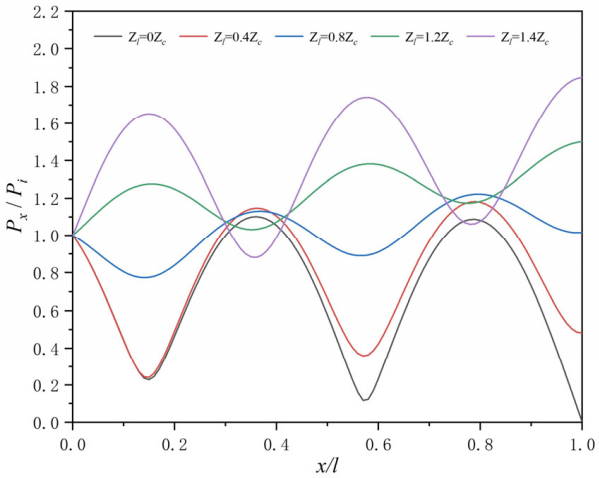

Figure 12. Wave amplitude distribution when the wave frequency is 1 Hz.

The wave frequency of the starting signal is 1 Hz. It can be seen that the wave amplitude of the pressure at any position in the tubular string is also fixed when the wave at the beginning is a periodic fluctuation state.

When $Z_l \neq Z_c$, the amplitude of the pressure wave in the tubular string fluctuates with the increasing x. Even zero can be observed at some positions, indicating that no fluctuation occurs at this position. Throughout the tubular string, the waves show a standing wave distribution. When the terminal impedance is smaller than the characteristic impedance, the ratio of the pressure head fluctuation is relatively small, while when the terminal impedance is larger than the characteristic impedance, the ratio of the pressure head fluctuation is relatively large.

Taking the terminal impedance $Z_l = Z_c$, the length of the tubular string is 3000 m. As shown in Figure 13, the tube resistance directly affects the magnitude of fluctuation amplitude in the tubular string, and the larger the peak value of fluctuation as the tube resistance R increases.

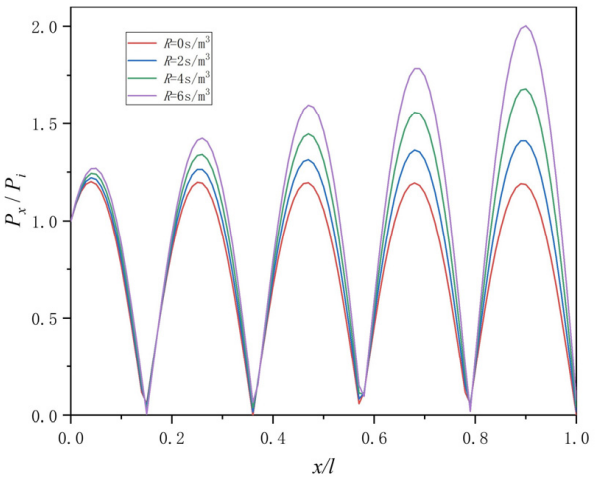

Figure 13. Effect of different tube resistances on fluctuations.

Taking the tube resistance as R = 24 s/m^3 and the length l as 1500 m, the distribution of the along-range fluctuation amplitude under the fluctuation frequency 1 Hz is shown in Figure 14. As the terminal impedance of the tube increases, the ratio peak of the pressure head fluctuation is larger and the hydraulic components with small terminal impedance reach the peak of fluctuation earlier than the hydraulic components with large terminal impedance.

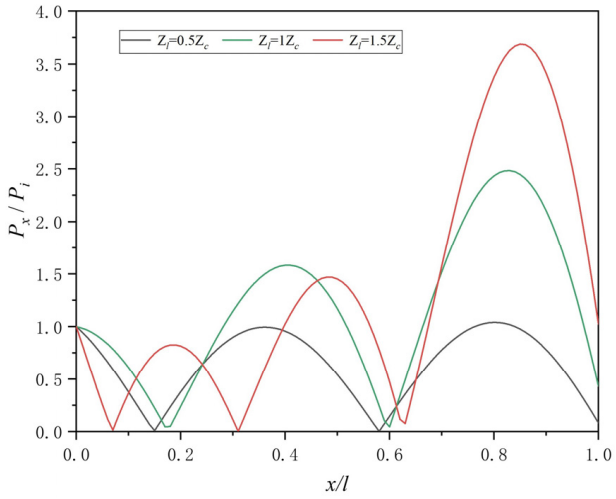

Figure 14. Effect of tube terminal impedance on fluctuations.

4.2. Frequency Response of the Tubular String

For Equation (30), only frequency f is kept variable (varying from 0.1 Hz to 20 Hz) under the conditions of the tube diameter 0.1 m, wave velocity 1260 m/s, fluid density 1200 kg/m^3, dynamic viscosity 3.81 $\times$ 10^{-3} Pa·s and terminal impedance $Z_l = 4Z_c$. Then the amplitude-frequency characteristics of the whole tubular string within 20 Hz can be calculated.

As seen in Figure 15, when the frequency of the signal gradually increases, multiple peaks can be observed, indicating that the signal is fluctuating. When the fluctuation frequency is very low, the ratio of the end amplitude to the beginning amplitude for the pressure head fluctuation is close to 1. When the length of the tubular string increases to 1000 m, the number of wave peaks increases and their amplitude becomes larger. For a short tubular string length of 100 m, the end amplitude showed multiple peaks over the entire frequency range, peaking at 3 Hz, 9 Hz and 16 Hz, and the end amplitude is greater than the beginning amplitude near all three frequency points. In deep wells, the ratio of the end amplitude to beginning amplitude fluctuates sharply as the signal frequency increases, and the signal frequency becomes more influential on the ratio of the end amplitude to beginning amplitude. If the interference signal is strong, the signal for communication is easily drowned in the interference signal, making it difficult to process the signal. Therefore, it is necessary to select the frequency corresponding to the peak of the ratio of the end amplitude to the beginning amplitude for signal transmission.

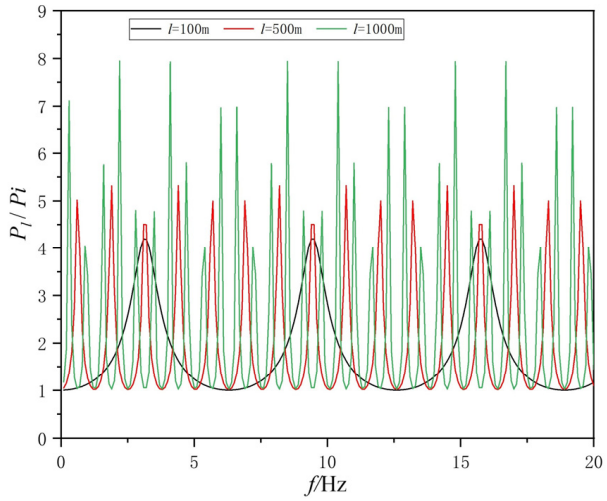

Figure 15. Amplitude-frequency characteristics of different lengths of tubular strings.

During the signaling of transient flow fluctuations, it is desirable that the signal has a relatively large amplitude after it has been transmitted to the surface. Since the well depth is always changing, the optimal communication frequency f is also always changing. For Equation (31), if the parameters other than tube length l and fluctuation frequency f are fixed, it is also possible to plot the amplitude–frequency space for different lengths of tubular strings, as shown in Figure 16. Once the length of the tubular string and the fluctuation frequency are determined, the corresponding amplitude ratio can be determined. If the signal processing capability of the ground equipment is limited and the signal is required to reach the ground with a higher amplitude, calculations can determine the appropriate frequency range for different lengths of tubular strings used for signal carriers.

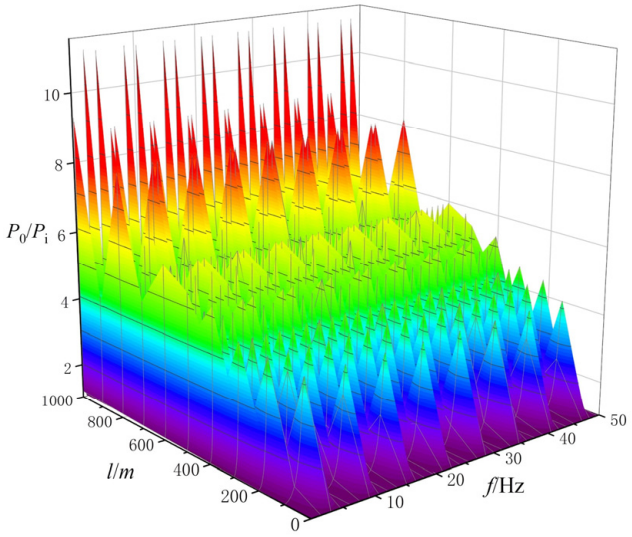

Figure 16. Amplitude–frequency space for different lengths of tubular strings.

5. Conclusions

In this paper, a matrix transfer model of transient flow wave in tubular strings and its transmission characteristics in stratified water injection are investigated. The effects of tubular string parameters and fluid properties on the waves of pressure and discharge are studied. The results show that:

(1) The transfer process of transient flow waves in a tubular string is studied, and a continuous transient flow wave transmission model based on transfer coefficient is proposed. The model defines the transfer coefficient to reflect the influence of tube size and fluid properties on the wave transmission and considers that the wave at any position in the tubular string can be regarded as the superposition of the wave in both directions along the tubular string. The analysis of the model shows that when one end of the tubular string is in the forced vibration state, the fluctuation in the tubular string shows a standing wave state. When the terminal impedance of the tubular string is small, the fluctuation amplitude in the tubular string is small. The model provides a powerful tool for analyzing the fluctuation wave in the tubular string. This study can provide clear insights into the use of transient flow waves for intelligent measurement and regulation and improve accurate control of downhole cableless intelligent water injection.

(2) An analytical method is proposed to calculate the transmission of fluctuations in the tubular string using a continuous transient flow wave transmission matrix model. The validity of the model based on the transfer matrix has been verified [32]. By analyzing the transmission of fluctuations, it is shown that the range of carrier frequencies suitable for communication is constantly changing as the well depth increases. Therefore, it is necessary to calculate the carrier frequency suitable for communication based on

specific parameters. The transfer matrix method allows a simple expression of the complex transmission process of wave signals in a tubular string. It is applicable to the analysis of wave signals in series tubular strings with various materials and sizes.

(3) The calculation methods of wave transmission velocity and wave attenuation are studied. The relationship between the influence of tubular string parameters and fluid characteristics on the wave transmission velocity and wave signal strength is obtained by simulation analysis. A two-layer stratified water injection test platform was built to study the fluctuation of discharge and pressure at monitoring points in the tubular string. The error of wave velocity was 0.69% and the error of wave signal amplitude was 3.85%, indicating the verifications of the calculation and simulation. The practical application of this work mainly provides theoretical support for the cable-free intelligent water injection technology of two-way signal transmission.

Author Contributions: Conceptualization, E.M.; data curation, L.Z.; formal analysis, J.Y.; funding acquisition, L.Z.; investigation, X.P.; methodology, E.M., C.L. and H.L.; project administration, H.L. and L.Z.; resources, L.Z. and X.P.; software, J.Y.; supervision, J.Y.; validation, J.Y. and X.P.; writing—original draft, C.L.; writing—review and editing, E.M., C.L. and H.L. All authors have read and agreed to the published version of the manuscript.

Funding: This work was supported by the China Institute of Petroleum Exploration and Development project (No. HYXY-ZB-2021-FW026).

Institutional Review Board Statement: Not applicable.

Informed Consent Statement: Not applicable.

Data Availability Statement: The data that support the findings of this study are available from the corresponding authors upon reasonable request.

Acknowledgments: The authors sincerely thank the anonymous reviewers who made valuable comments on this paper.

Conflicts of Interest: The authors declare that they have no known competing financial interests or personal relationships that could have appeared to influence the work reported in this paper.

Nomenclature

A	Area of the tube, (m^2)
a	Velocity of the pressure wave, (m/s)
g	Acceleration due to gravity, (kg/m^3)
t	Time, (s)
x	distance, (m)
V	velocity, (m/s)
λ	Darcy–Weisbach friction coefficient, dimensionless
D	Diameter of the tube, (m)
x	Distance along the tube, (m)
j	Plural, $j^2 = -1$
β	Angle between the tubular string and the horizontal plane, (rad)
Q	Discharge, (m^3/s)
Q_0	Mean discharge, (m^3/s)
Q'	Discharge deviation from the mean, (m^3/s)
H	Pressure head, (m)
H_0	Mean pressure head, (m)
H'	Pressure head deviation from the mean, (m)
K	Elasticity modulus of the fluid, (MPa)
E	Young modulus of the tube material, (MPa)
e	Thickness of the tube, (m)
ρ_l	Liquid density, (kg/m^3)

ρ_g	Gas density, (kg/m^3)
ρ	Fluid density, (kg/m^3)
β_g	Volumetric gas content, (%)
K_l	Liquid bulk modulus of elasticity, (Pa)
K_g	Gas bulk modulus of elasticity
m	Specific heat ratio of the gas
ψ	Parameter depends on the tube geometry and constraint conditions
s	Transmission distance when the signal attenuates to the source strength 1/e, (m)
f	Frequency of the signal, (Hz)
ω	Viscosity of the transmission fluid, (Pa·s)

References

1. Aljuboori, F.A.; Lee, J.H.; Elraies, K.A.; Stephen, K.D. Using Low Salinity Waterflooding to Improve Oil Recovery in Naturally Fractured Reservoirs. *Appl. Sci.* **2020**, *10*, 4211. [CrossRef]
2. Hu, B.; Gu, Z.; Zhou, C.; Wang, L.; Huang, C.; Su, J. Investigation of the Effect of Capillary Barrier on Water–Oil Movement in Water Flooding. *Appl. Sci.* **2022**, *12*, 6285. [CrossRef]
3. Almeida, L.F.; Túpac, Y.J.; Lazo, J.G.L.; Pacheco, M.A.; Vellasco, M.M.B.R. Evolutionary Optimization of Smart-Wells Control under Technical Uncertainties. In Proceedings of the SPE Latin American & Caribbean Petroleum Engineering Conference, Buenos Aires, Argentina, 15–18 April 2007; Volume 3, pp. 1199–1205. [CrossRef]
4. Zhang, L.; Xu, C.; Zhang, K.; Yao, C.; Yang, Y.; Yao, J. Production Optimization for Alternated Separate-Layer Water Injection in Complex Fault Reservoirs. *J. Pet. Sci. Eng.* **2020**, *193*, 107409. [CrossRef]
5. Li, C.; Lan, H.; An, R. Simulation on Adjustment Ability of Adjustable Water Nozzle in Separate-Layer Water Injection. *Pet. Sci. Technol.* **2023**, *41*, 1–25. [CrossRef]
6. Liu, H.; Pei, X.; Jia, D.; Sun, F.; Guo, T. Connotation, Application and Prospect of the Fourth-Generation Separated Layer Water Injection Technology. *Pet. Exp. Dev.* **2017**, *44*, 644–651. [CrossRef]
7. Che, T.C.; Duan, H.F.; Lee, P.J. Transient Wave-Based Methods for Anomaly Detection in Fluid Pipes: A Review. *Mech. Syst. Signal Process.* **2021**, *160*, 107874. [CrossRef]
8. Yuan, Z.; Deng, Z.; Jiang, M.; Xie, Y.; Wu, Y. A Modeling and Analytical Solution for Transient Flow in Natural Gas Pipelines with Extended Partial Blockage. *J. Nat. Gas Sci. Eng.* **2015**, *22*, 141–149. [CrossRef]
9. Wang, X.-J.; Lambert, M.F.; Simpson, A.R.; Liggett, J.A.; Vıtkovský, J.P. Leak Detection in Pipelines Using the Damping of Fluid Transients. *J. Hydraul. Eng.* **2002**, *128*, 697–711. [CrossRef]
10. Liu, C.; Li, Y.; Xu, M. An Integrated Detection and Location Model for Leakages in Liquid Pipelines. *J. Pet. Sci. Eng.* **2019**, *175*, 852–867. [CrossRef]
11. Cheng, Z.; Xu, Y.; Gu, C.; Liu, Z. Research on Pressure Wave and Communication of Realtime Testing and Adjustable System in Oilfield Layered Water Injection. In Proceedings of the 2018 International Conference on Intelligent Medical & International Conference on Transportation and Traffic, Beijing, China, 21–23 December 2018; pp. 208–212. [CrossRef]
12. Li, Y.; Hu, X.; Zhou, F.; Qiu, Y.; Li, Z.; Luo, Y. A New Comprehensive Filtering Model for Pump Shut-in Water Hammer Pressure Wave Signals during Hydraulic Fracturing. *J. Pet. Sci. Eng.* **2022**, *208*, 109796. [CrossRef]
13. Liu, H.; Zheng, L.; Yu, J.; Ming, E.; Yang, Q.; Jia, D.; Cao, G. Development and Prospect of Downhole Monitoring and Data Transmission Technology for Separated Zone Water Injection. *Pet. Exp. Dev.* **2023**, *50*, 191–201. [CrossRef]
14. Joukowski, N.E. Memoirs of the Imperial Academy Society of St. Petersburg. *Proc. Am. Water Work. Assoc.* **1898**, *24*, 341–424.
15. Allievi, L. Teoria Generale Del Moto Perturbato Dell'acqua Nei Tubi in Pressione. Ann. Della Soc. Degli Ing. ed Archit. Ital. (English translation, Halmos, E.E: Theory of Water Hammer, American Society of Mechanical Engineering, 1925). 1902. Available online: https://cir.nii.ac.jp/crid/1572824499859986304 (accessed on 14 February 2023).
16. Wood, F.M. The Application of Heaviside's Operational Calculus to the Solution of Problems in Water Hammer. *Trans. Am. Soc. Mech. Eng.* **1937**, *59*, 707–713. [CrossRef]
17. Wylie, E.B.; Streeter, V.L.; Suo, L. *Fluid Transients in Systems*; Prentice Hall: Englewood Cliffs, NJ, USA, 1993; Volume 1.
18. Ham, A.A. On the Dynamics of Hydraulic Lines Supplying Servosystems. Ph.D. Thesis, Technical University of Delft, Delft, The Netherlands, 1982.
19. Qiu, Y.; Hu, X.; Zhou, F.; Li, Z.; Li, Y.; Luo, Y. Water Hammer Response Characteristics of Wellbore-Fracture System: Multi-Dimensional Analysis in Time, Frequency and Quefrency Domain. *J. Pet. Sci. Eng.* **2022**, *213*, 110425. [CrossRef]
20. Hou, Y.; Peng, Y.; Chen, Z.; Liu, Y.; Zhang, G.; Ma, Z.; Tian, W. Investigation on the Controlling Factors of Pressure Wave Propagation Behavior Induced by Pulsating Hydraulic Fracturing. *SPE J.* **2021**, *26*, 2716–2735. [CrossRef]
21. Afshar, M.H.; Rohani, M. Water Hammer Simulation by Implicit Method of Characteristic. *Int. J. Press. Vessel. Pip.* **2008**, *85*, 851–859. [CrossRef]
22. Kandil, M.; Kamal, A.M.; El-Sayed, T.A. Effect of Pipematerials on Water Hammer. *Int. J. Press. Vessel. Pip.* **2020**, *179*, 103996. [CrossRef]
23. Garg, R.K.; Kumar, A. Experimental and Numerical Investigations of Water Hammer Analysis in Pipeline with Two Different Materials and Their Combined Configuration. *Int. J. Press. Vessel. Pip.* **2020**, *188*, 104219. [CrossRef]

24. Urbanowicz, K.; Stosiak, M.; Towarnicki, K.; Bergant, A. Theoretical and Experimental Investigations of Transient Flow in Oil-Hydraulic Small-Diameter Pipe System. *Eng. Fail. Anal.* **2021**, *128*, 105607. [CrossRef]
25. Wu, D.; Yang, S.; Wu, P.; Wang, L. MOC-CFD Coupled Approach for the Analysis of the Fluid Dynamic Interaction between Water Hammer and Pump. *J. Hydraul. Eng.* **2015**, *141*, 6015003. [CrossRef]
26. Haghighi, A.; Shamloo, H. Transient Generation in Pipe Networks for Leak Detection. *Proc. Inst. Civ. Eng. Water Manag.* **2011**, *164*, 311–318. [CrossRef]
27. Fu, H.; Wang, S.; Ling, K. Detection of Two-Point Leakages in a Pipeline Based on Lab Investigation and Numerical Simulation. *J. Pet. Sci. Eng.* **2021**, *204*, 108747. [CrossRef]
28. Wang, X.; Hovem, K.; Moos, D.; Quan, Y. Water Hammer Effects on Water Injection Well Performance and Longevity. In Proceedings of the SPE International Symposium and Exhibition on Formation Damage Control, Lafayette, LA, USA, 13–15 February 2008; Volume 1, pp. 224–232. [CrossRef]
29. Choi, S.K.; Huang, W.S. Impact of Water Hammer in Deep Sea Water Injection Wells. In Proceedings of the SPE Annual Technical Conference and Exhibition, Denver, CO, USA, 30 October–2 November 2011; Volume 2, pp. 1319–1332. [CrossRef]
30. Bouchaala, F.; Ali, M.Y.; Matsushima, J. Compressional and Shear Wave Attenuations from Walkway VSP and Sonic Data in an Offshore Abu Dhabi Oilfield. *Comptes Rendus Géosci.* **2021**, *353*, 337–354. [CrossRef]
31. Meniconi, S.; Brunone, B.; Ferrante, M.; Capponi, C. Mechanism of Interaction of Pressure Waves at a Discrete Partial Blockage. *J. Fluids Struct.* **2016**, *62*, 33–45. [CrossRef]
32. Chaudhry, M.H. *Applied Hydraulic Transients*; Springer: Berlin/Heidelberg, Germany, 2014; Volume 415, pp. 31–42.
33. Kandil, M.; Kamel, A.; El-Sayed, M. Analytical and CFD Analysis Investigation of Fluid-Structure Interaction during Water Hammer for Straight Pipe Line. *Int. J. Press. Vessel. Pip.* **2021**, *194*, 104528. [CrossRef]
34. Zhang, H.M.; Zhang, L.X. Numerical Simulation of Fluid-Structure Interaction with Water Hammer in a Vertical Penstock Subjected to High Water Head. *Adv. Mater. Res.* **2014**, *860–863*, 1530–1534. [CrossRef]
35. Matsushima, J.; Ali, M.Y.; Bouchaala, F. A Novel Method for Separating Intrinsic and Scattering Attenuation for Zero-Offset Vertical Seismic Profiling Data. *Geophys. J. Int.* **2017**, *211*, 1655–1668. [CrossRef]
36. Bouchaala, F.; Ali, M.Y.; Farid, A. Estimation of Compressional Seismic Wave Attenuation of Carbonate Rocks in Abu Dhabi, United Arab Emirates. *Comptes Rendus Geosci.* **2014**, *346*, 169–178. [CrossRef]
37. Paganoni, M.; Cartwright, J.A.; Foschi, M.; Shipp, R.C.; Van Rensbergen, P. Structure II Gas Hydrates Found below the Bottom-simulating Reflector. *Geophys. Res. Lett.* **2016**, *43*, 5696–5706. [CrossRef]